AMERICAN SOCIETY FOR MICROBIOLOGY | Applied and Environmental Microbiology®

ENZYMOLOGY AND PROTEIN ENGINEERING

A Phage Lysin Fused to a Cell-Penetrating Peptide Kills Intracellular Methicillin-Resistant *Staphylococcus aureus* in Keratinocytes and Has Potential as a Treatment for Skin Infections in Mice

ZhaoFei Wang,[a] LiCheng Kong,[a] Yang Liu,[a] Qiang Fu,[a] ZeLin Cui,[b] Jian Wang,[c] JingJiao Ma,[a] HengAn Wang,[a] YaXian Yan,[a] JianHe Sun[a]

[a]School of Agriculture and Biology, Shanghai Jiao Tong University, Shanghai Key Laboratory of Veterinary Biotechnology, Key Laboratory of Urban Agriculture (South), Ministry of Agriculture, Shanghai, People's Republic of China

[b]Department of Laboratory Medicine, Shanghai General Hospital, Shanghai Jiao Tong University School of Medicine, Shanghai, People's Republic of China

[c]Shanghai Animal Disease Control Centre, Shanghai, People's Republic of China

ABSTRACT *Staphylococcus aureus* is the main pathogen that causes skin and skin structure infections and is able to survive and persist in keratinocytes of the epidermis. Since the evolution of multidrug-resistant bacteria, the use of phages and their lysins has presented a promising alternative approach to treatment. In this study, a cell wall hydrolase (also called lysin) derived from *Staphylococcus* phage JD007 (JDlys) was identified. JDlys showed strong lytic activity against methicillin-resistant *Staphylococcus aureus* (MRSA) strains from different sources and of different multilocus sequence typing (MLST) types. Furthermore, a fusion protein consisting of a cell-penetrating peptide derived from the *trans*-activating transcription (Tat) factor fused to JDlys (CPP_{Tat}-JDlys) was used to kill MRSA bacteria causing intracellular infections. CPP_{Tat}-JDlys, in which the fusion of CPP_{Tat} to JDlys had almost no effect on the bacteriolytic activity of JDlys, was able to effectively eliminate intracellular MRSA bacteria and alleviate the inflammatory response and cell damage caused by MRSA. Specifically, CPP_{Tat}-JDlys was able to combat MRSA-induced murine skin infections and, consequently, expedite the healing of cutaneous abscesses. These data suggest that the novel antimicrobial CPP-JDlys may be a worthwhile candidate as a treatment for skin and skin structure infections caused by MRSA.

IMPORTANCE *S. aureus* is the main cause of skin and skin structure infections due to its ability to invade and survive in the epithelial barrier. Due to the overuse of antibiotics in humans and animals, *S. aureus* has shown a high capacity for acquiring and accumulating mechanisms of resistance to antibiotics. Moreover, most antibiotics are usually limited in their ability to overcome the intracellular persistence of bacteria causing skin and skin structure infections. So, it is critical to seek a novel antimicrobial agent to eradicate intracellular *S. aureus*. In this study, a cell-penetrating peptide fused to lysin (CPP-JDlys) was engineered. Our results show that CPP-JDlys can enter keratinocytes and effectively eliminate intracellular MRSA. Meanwhile, experiments with mice revealed that CPP-JDlys efficiently inhibits the proliferation of MRSA in murine skin and thus shortens the course of wound healing. Our results indicate that the CPP-fused lysin has potential for use for the treatment of skin infections caused by MRSA.

KEYWORDS *Staphylococcus aureus*, lysin, cell-penetrating peptide, keratinocytes, skin infection

Received 14 February 2018 **Accepted** 3 April 2018

Accepted manuscript posted online 6 April 2018

Citation Wang Z, Kong L, Liu Y, Fu Q, Cui Z, Wang J, Ma J, Wang H, Yan Y, Sun J. 2018. A phage lysin fused to a cell-penetrating peptide kills intracellular methicillin-resistant *Staphylococcus aureus* in keratinocytes and has potential as a treatment for skin infections in mice. Appl Environ Microbiol 84:e00380-18. https://doi.org/10.1128/AEM.00380-18.

Editor Robert M. Kelly, North Carolina State University

Address correspondence to JianHe Sun, sunjhe@sjtu.edu.cn.

Healthy skin provides a unique ecological environment and immunological barrier against pathogenic microorganisms, especially *Staphylococcus aureus*, which is the main cause of skin and skin structure infections (SSSIs) (1, 2). Keratinocytes are the major cell type in the epidermis and actively participate in and orchestrate the innate immune response of the skin (3). Recent studies have illuminated that, like immune cells, keratinocytes are initial sensors for skin and important producers of antimicrobial peptides and proinflammatory cytokines at the preliminary stage of an *S. aureus* infection (4–6). However, evidence indicates that *S. aureus* bacteria have the ability to survive in keratinocytes, where they might escape the immune response, leading to persistent infection in the skin (7, 8). It is known that the efficacy of the majority of antimicrobial agents is restricted by the cutaneous intracellular accumulation of *S. aureus* because most antibiotics hardly enter eukaryotic cells freely and micromolecule antimicrobial peptides disrupt the balance of the microbiota colonizing the skin since they possess a broad spectrum of activity (9, 10). Moreover, the overuse of antibiotics in humans and animals has increased the selection of resistant *S. aureus* strains. As a result, a mass of *S. aureus* strains (e.g., methicillin-resistant *S. aureus* [MRSA]) has been declared to be resistant to various antimicrobials (11).

As a potential alternative or complement to current antimicrobial agents (i.e., antibiotics), phage therapy has been drawing more and more attention as a strategy to treat MRSA infections (12, 13). The potent bactericidal effect of phages is mainly attributed to their genome-encoded cell wall hydrolase, also called lysin, which exhibits a lethal effect by forming holes in the cell wall through peptidoglycan digestion (14). Evidence has shown that lysins exhibit a high level of antibacterial activity, and they have proven their effectiveness for the treatment of infections caused by bacteria resistant to conventional chemical antibiotics in diverse animal models (15–17). A number of studies have revealed the enormous potential of the use of phage lysins, which even surpasses that of intact phage, as therapeutics for MRSA infections (16, 18).

Despite the immense potential of lysins for eradicating infections caused by drug-resistant strains, until now, only a few clinical trials of lysins have been carried out in humans. The main reason for this is that when they are administered systemically, the lysins trigger an immune response, leading to the production of antibodies, which can drastically reduce the effectiveness of the antimicrobial treatment (14, 19). Moreover, lysins are rarely relied on to get rid of intracellular bacteria because they do not possess the ability to penetrate eukaryotic cells (14, 20). So far, many studies have disclosed that cell-penetrating peptides (CPPs) are short peptides that are able to penetrate biological membranes and drive the bioactive cargo into the cells by internalization (21–23). Specifically, many types of drugs have been transported into cells using CPPs, including antisense oligonucleotides, small-molecule pharmaceuticals, and therapeutic proteins (24). Given this, in this study a lysin from phage JD007 (JDlys) fused to CPP (CPP-JDlys) was constructed to facilitate JDlys entry into keratinocytes, and its ability to inhibit the proliferation of *S. aureus* in murine skin and, consequently, shorten the course of wound healing was demonstrated.

RESULTS

Characterization of staphylococcal lysin derived from phage JD007. A previous study demonstrated that phage JD007 exhibits strong antibacterial activity against various types of *S. aureus* strains (25). In this study, a lysin was identified from the whole-genome sequence of phage JD007 (JDlys). Cloning, prokaryotic expression, and purification of JDlys were carried out as detailed in Materials and Methods. The purified JDlys was approximately 57 kDa, according to sodium dodecyl sulfate polyacrylamide gel electrophoresis (SDS-PAGE) (see Fig. S1 in the supplemental material). To examine the bacteriolytic activity of JDlys against *Staphylococcus*, a MIC assay was performed. As shown in Table 1, JDlys was able to inhibit the growth of *Staphylococcus* strains from different sources and of different multilocus sequence typing (MLST) types.

Construction and bactericidal activity of the CPP-JDlys fusion protein. In order to enable the JDlys entering eukaryotic cells to combat intracellular *S. aureus*, three

TABLE 1 The various strains used in this study and lytic activity of JDlys and CPP-JDlys

Species	Strain	MLST type	MIC (μg/ml)				Source[a]
			Jdlys	CPP_{Tat}-JDlys	CPP_{Ant}-JDlys	CPP_{TP10}-JDlys	
Methicillin-resistant	USA300	ST[b] 8	20	40	160	160	III
Staphylococcus aureus	MS5	ST 5	10	10	160	160	I
	MS6	ST 5	20	40	320	320	I
	MS8	ST 9	20	20	—[c]	320	I
	MS10	ST 239	80	80	—	—	I
	MS11	ST 9	20	40	320	320	I
	MS15	ST 5	20	40	320	160	I
	MS16	ST 9	20	40	320	320	I
	MS17	ST 398	80	80	—	—	I
	MS19	ST 9	10	20	320	320	I
	MS20	ST 398	20	20	—	160	I
	MS21	ST 398	20	40	—	—	I
Methicillin-susceptible	ATCC 25923	ST 243	20	40	160	160	III
Staphylococcus aureus	ATCC 29213	ST 5	40	40	320	320	III
	S1	ST 398	80	80	—	—	I
	S2	ST 239	20	20	160	160	I
	S4	ST 239	20	20	320	160	I
	S5	ST 398	10	20	160	160	I
	SH-5	ST 9	20	20	320	160	II
	SH-6	ST 9	40	40	—	320	II
Staphylococcus sciuri	Sci-3		40	40	320	320	II
Staphylococcus saprophyticus	Sap-1		40	80	—	—	II
Staphylococcus caseolyticus	Cas-1		80	80	320	320	II

[a]I, clinically isolated pathogenic strains; II, strains isolated from milk samples of dairy cows with mastitis; III, purchased from the American Type Culture Collection.
[b]ST, sequence type.
[c]—, no antimicrobial activity.

kinds of CPPs were fused to either the amino terminus or the carboxy terminus of JDlys (Table 2). The results of analysis of the bactericidal effect showed that CPP_{Tat}-JDlys (where CPP_{Tat}, the CPP derived from the *trans*-activating transcription [Tat] factor of human immunodeficiency virus type 1, was fused to the amino terminus of JDlys) presented the same antibacterial spectrum as JDlys, although CPP_{Tat}-JDlys showed reduced a bactericidal effect against a small proportion of strains compared with that of JDlys (Table 1). However, CPP_{Ant}-JDlys (where CPP_{Ant}, the CPP derived from the *Antennapedia* homeodomain of *Drosophila*, was fused to the amino terminus of JDlys) and CPP_{TP10}-JDlys (where CPP_{TP10}, the CPP derived from the shorter analog of transportan, was fused to the amino terminus of JDlys) exhibited significantly reduced bactericidal effects against a large proportion of strains. Unfortunately, JDlys completely lost its bactericidal effect after it was fused to any of the three kinds of CPPs at the carboxy terminus (data not shown).

Intracellular killing activity of CPP-JDlys. Previous research found that certain *S. aureus* strains exhibit an ability to adhere to and invade eukaryotic cells (26). Here, our research showed that MRSA strain USA300 had a relatively strong ability to adhere to and invade HaCaT keratinocytes (Fig. S2). To investigate the activities of the various CPP-JDlys constructs against intracellular MRSA strains, HaCaT keratinocytes were infected with USA300 and subsequently treated with JDlys and the three CPP-JDlys constructs (where the CPPs were fused to the amino terminus of JDlys). CPP_{Tat}-JDlys exhibited a greater ability to kill intracellular MRSA strains than JDlys, indicating that

TABLE 2 Amino acid sequences of CPPs

CPP	Sequence	Reference
CPP_{Tat}	YGRKKRRQRRR	21
CPP_{Ant}	RQIKIWFQNRRMKWKK	22
CPP_{TP10}	AGYLLGKINLKALAALAKKIL	23

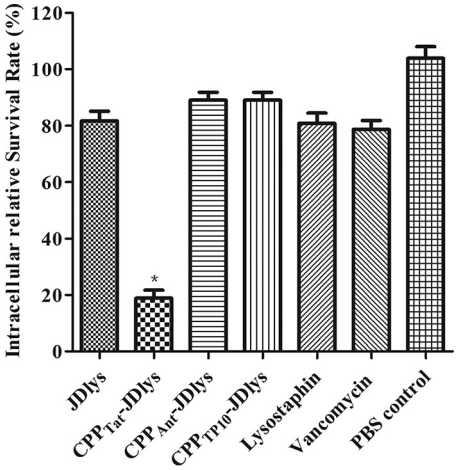

FIG 1 Elimination of intracellular MRSA in HaCaT keratinocytes. Keratinocytes were infected, treated with gentamicin to kill the extracellular *S. aureus*, and then treated with purified JDlys, CPP-JDlys, commercial lysostaphin, or vancomycin. Infected cells were treated with PBS as a control. *, the intracellular bacterial numbers after treatment with CPP_{Tat}-JDlys were significantly lower ($P < 0.05$) than those after the other treatments. The data shown are means ± SEMs from at least three independent experiments.

CPP_{Tat} could deliver JDlys into keratinocytes so that it could exert its activity against intracellular bacteria (Fig. 1 and S3). However, neither CPP_{Ant}-JDlys nor CPP_{Tp10}-JDlys could eliminate intracellular MRSA. Previous evidence showed that chloramphenicol (Cm) has the ability to kill intracellular *S. aureus* (27). However, the result showed that 80 μg/ml (2× MIC) of CPP_{Tat}-JDlys had a bactericidal effect in keratinocytes similar to that of 100 μg/ml (8× MIC) of chloramphenicol (Fig. S3).

The levels of proinflammatory cytokines and cytotoxicity can be used to assess the severity of the effect of an infection with an intracellular pathogen on eukaryotic cells. Our study found that treatment with CPP_{Tat}-JDlys decreased the amounts of tumor necrosis factor alpha (TNF-α), interleukin-6 (IL-6), and lactate dehydrogenase (LDH) released compared with the amounts released after treatment with JDlys and vancomycin. This demonstrates that treatment with CPP_{Tat}-JDlys can alleviate the inflammation and reduce the cytotoxicity caused by intracellular *S. aureus* (Fig. 2A and B).

To determine whether CPP_{Tat}-JDlys transferred across the keratinocyte membrane, keratinocytes were exposed to fluorescently labeled CPP_{Tat}-JDlys (green) and fluorescently labeled MRSA strain USA300 (red) and monitored in real time by confocal microscopy. USA300 and the CPP_{Tat}-JDlys were identified to be intracellularly colocalized (yellow) in a single *z* plane within the keratinocytes (Fig. 3).

Activity of CPP_{Tat}-JDlys in a mouse model of cutaneous abscesses. To validate the bactericidal efficacy of CPP_{Tat}-JDlys against local infections, mice were subcutaneously infected with MRSA and treated with proteins over the course of 3 days. The efficacy of CPP_{Tat}-JDlys was measured by the use of multiple parameters, as described below.

Over 13 days, CPP_{Tat}-JDlys treatment significantly restricted the area of the abscess caused by USA300 compared with that in control mice treated with medium only (Fig. 4 and 5). The maximum area of the abscess at day 5 after treatment with CPP_{Tat}-JDlys was about 0.72 cm^2, which was significantly smaller than that in the medium-treated controls (about 2.68 cm^2 at day 11) (Fig. 5). Furthermore, the CPP_{Tat}-JDlys-treated group exhibited a relatively smaller area of the abscess at days 3, 5, and 7 (about 0.44 cm^2, 0.72 cm^2, and 0.57 cm^2, respectively) than the JDlys-treated group (about 0.88 cm^2, 1.23 cm^2, and 1.08 cm^2, respectively). As a critical assessment of CPP_{Tat}-JDlys's efficacy, the number of CFU per abscess was determined in the mice. The result showed that the number of bacterial CFU from the abscesses was obviously lower for CPP_{Tat}-JDlys-treated mice than for JDlys-treated mice (almost 10-fold lower) and medium-treated mice (more than 100-fold lower) at every time point (Fig. 6). The substantial reductions

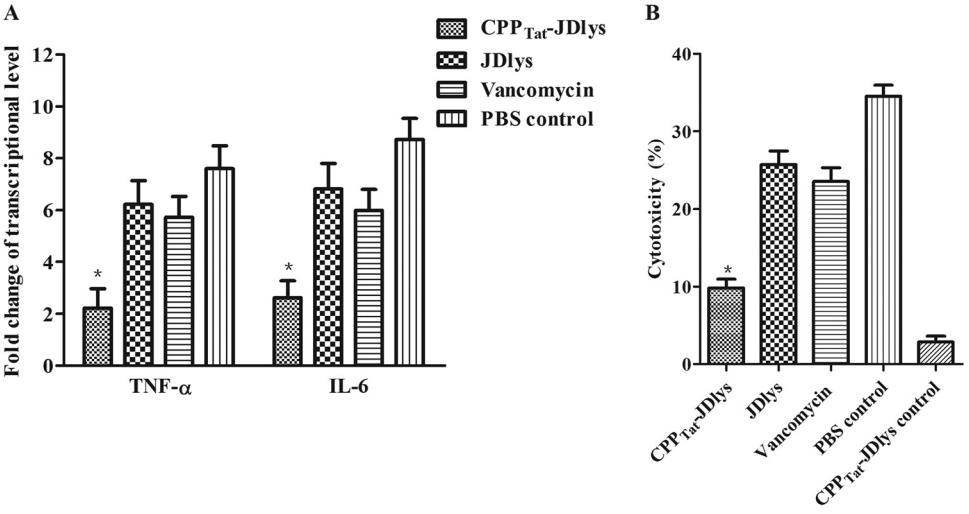

FIG 2 Intracellular MRSA-induced cytokine expression and cytotoxicity in HaCaT keratinocytes. Keratinocytes were infected, treated with gentamicin to kill the extracellular *S. aureus*, and then treated with purified CPP$_{Tat}$-JDlys, JDlys proteins, or vancomycin. Infected cells were treated with PBS as a control. (A) The mRNA levels of TNF-α and IL-6 were measured by real-time PCR at 3 h after the treatments mentioned above. The levels of TNF-α and IL-6 mRNA were normalized to the levels of β-actin mRNA and then were expressed as the *n*-fold increases with respect to the levels in uninfected cells. (B) Effect of bacterial cell-mediated cytotoxicity measured by LDH cytotoxicity assays. Infected cells were treated with PBS as a control. Uninfected cells were treated with CPP$_{Tat}$-JDlys as a CPP$_{Tat}$-JDlys control. *, the cytokine levels or cytotoxicity for samples treated with CPP$_{Tat}$-JDlys were significantly lower ($P < 0.05$) than those for samples treated with JDlys, vancomycin, and the PBS control. The data shown are means ± SEMs from at least three independent experiments.

in the number of CFU associated with CPP$_{Tat}$-JDlys were congruent with the observed reductions in the area of the abscess (Fig. 5).

The strength and efficiency of the host immune response depend on the level of proinflammatory cytokines, including TNF-α and IL-6, which are indicators of the severity of skin infections (28, 29). In this study, the levels of proinflammatory cytokines (TNF-α and IL-6) in the abscess tissues were measured by the use of cytokine enzyme-linked immunosorbent assay (ELISA) kits. The magnitudes of the TNF-α and IL-6 responses in the CPP$_{Tat}$-JDlys-treated mice were significantly greater in the early stages (before day 6) of treatment but decreased rapidly over time (Fig. 7). Conversely, for the medium-treated mice, the levels of cytokines increased gradually over time, indicating that CPP$_{Tat}$-JDlys effectively inhibited the inflammation due to MRSA on the skin surface. Interestingly, the levels of proinflammatory cytokines in the Cm-treated mice were higher than those in the CPP$_{Tat}$-JDlys-treated mice at every time point (Fig. 7). However, there was no difference in the abscess size or the number of bacterial CFU between the two treated groups (Fig. 4 to 6). Moreover, both groups of uninfected mice treated with JDlys and CPP$_{Tat}$-JDlys exhibited proinflammatory cytokine levels similar to those in the PBS-treated control group.

Histopathological assays of the abscess tissues were carried out at 5 and 8 days after treatment with CPP$_{Tat}$-JDlys. Skin lesions from untreated (medium-treated) mice exhibited extensive epidermal and soft tissue necrosis after 5 days. As time went on, an undiminished infection with a large abscess and inflammatory cell infiltration emerged in these mice (Fig. 8), whereas CPP$_{Tat}$-JDlys-treated mice showed relatively moderate epidermal necrosis and cellulitis after 5 days. After 8 days, the epidermis was regenerating rapidly and the wound was healing gradually (Fig. 8).

DISCUSSION

S. aureus is the major cause of SSSIs and has the ability to invade and survive in distinctly differentiated keratinocytes (1, 3). However, the intracellular persistence of the bacteria in SSSIs contributes to the difficulty of antibiotic treatment, especially in MRSA infections (30, 31). So, it is critical to seek a novel antimicrobial agent that has the excellent properties of high selectivity and specificity to eradicate intracellular *S. aureus*.

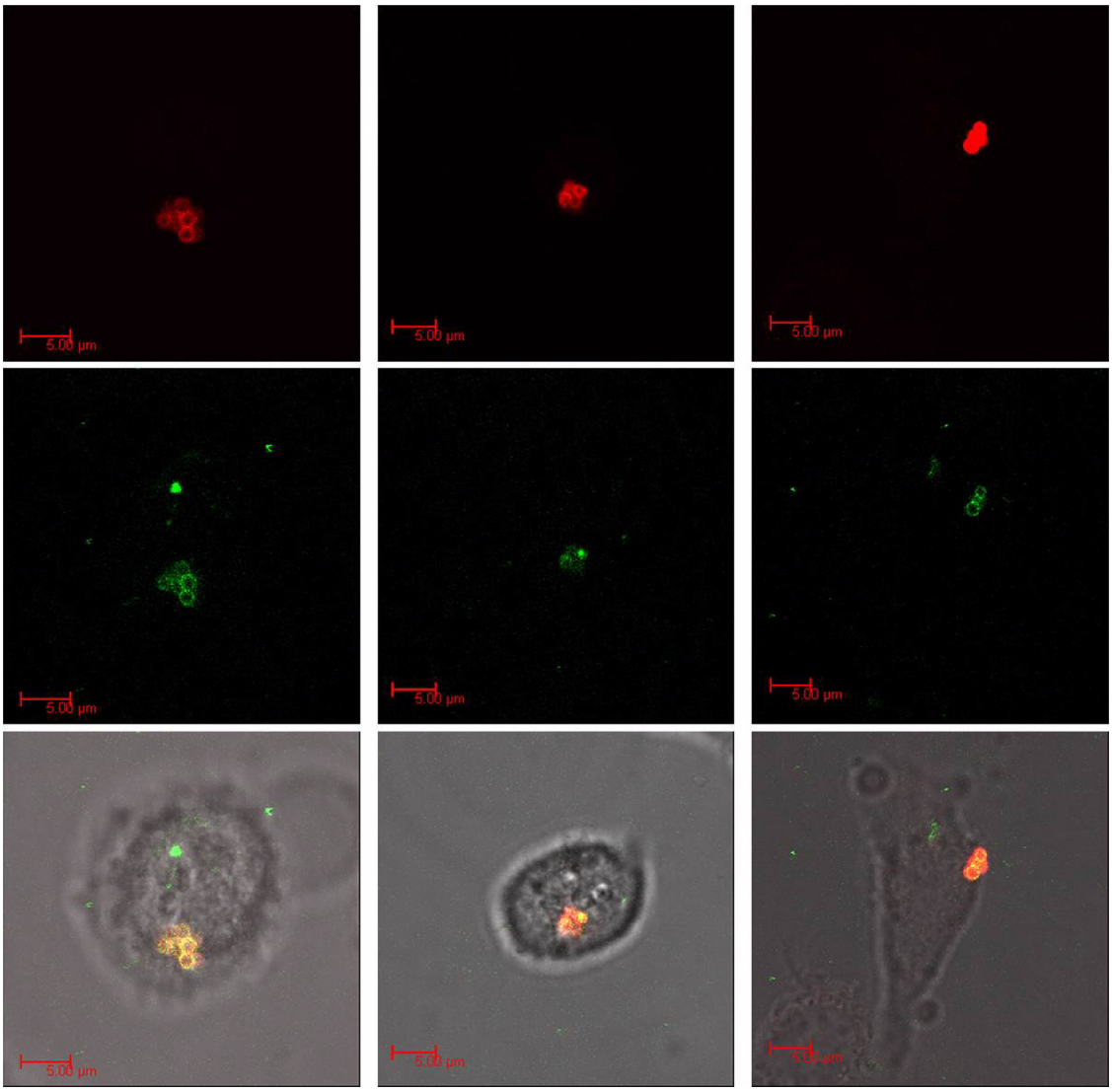

FIG 3 Confocal microscopy images of infected HaCaT keratinocytes treated with CPP-JDlys. Keratinocytes were exposed to fluorescently labeled CPP_{Tat}-JDlys (green; middle row) and fluorescently labeled MRSA strain USA300 (red; top row) and monitored in real time by confocal microscopy. *S. aureus* bacteria were colocalized with CPP_{Tat}-JDlys (yellow) in the combined panels in the bottom row. Images of the three columns are representative of three independent experiments.

Lysins have been broadly investigated as potential antimicrobial agents in recent years (15, 32). However, when used alone and/or without modification, it is difficult for lysins to kill intracellular pathogens (14). In order to address this concern, three kinds of CPPs which could deliver the cargo into eukaryotic cells were fused with JDlys (21–23). However, when the CPPs were fused at the carboxy terminus of JDlys, the ability of the three kinds of fusion proteins to lyse *S. aureus in vitro* was completely inactivated. Numerous researchers have demonstrated that the cell wall binding domain of lysins (usually in the carboxy terminus of lysins) plays a pivotal role in the ability of lysins to recognize their substrates (bacterial cell wall peptidoglycan) (14). In addition, the lysin might lose bactericidal activity once the binding domain is destroyed (32, 33). Therefore, it is presumed that CPPs fused to the carboxy terminus of lysins might influence the activity of JDlys by interfering with the cell wall binding domain in the carboxy terminus. Fortunately, JDlys fused with the three kinds of CPPs at the amino terminus retained bactericidal activity. Further, we confirmed that CPP_{Tat}, which fused to the amino terminus of JDlys, could deliver the cargo (JDlys) into keratinocytes, which is in accordance with the findings of Johnson et al. (21). Meanwhile, our results

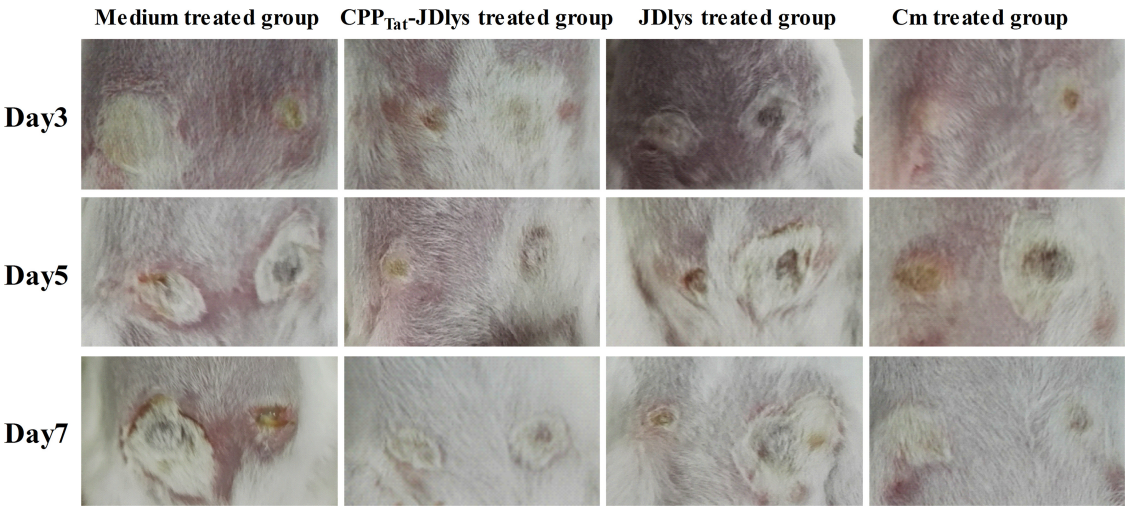

FIG 4 Restriction of the dermonecrotic area and the severity of dermonecrosis at days 3, 5, and 7 in the mouse model. Images of the dermonecrotic areas in the medium control-, CPP$_{Tat}$-JDlys-, JDlys-, and Cm-treated mice are shown and are representative of those from three experiments. Note the smaller areas of dermonecrosis and the faster healing of lesions in CPP$_{Tat}$-JDlys-treated mice than in the control mice, in which the lesions remained exudative.

indicated that CPP$_{Tat}$-JDlys is able to eliminate intracellular bacteria effectively and alleviate the MRSA-induced inflammatory response and cell damage (Fig. 1 and 2). However, neither CPP$_{Ant}$-JDlys nor CPP$_{TP10}$-JDlys was able to eliminate intracellular MRSA effectively. The possible reason may be that the cell-penetrating ability of CPP$_{Ant}$ and CPP$_{TP10}$ was inhibited by the advanced structure of the JDlys protein. Further studies are needed to evaluate this possibility.

As a main constituent in the epidermis, keratinocytes can provide a shelter for pathogens to evade immune defenses, and thus, pathogens, especially *S. aureus*, inflict persistent damage to the skin (34). Previously, we revealed that CPP$_{Tat}$-JDlys is capable of penetrating the membrane of keratinocytes to eliminate intracellular bacteria. Wang et al. revealed that a cell-penetrating peptide (which has an amino acid sequence similar to that of CPP$_{Tat}$) could deliver the drug through the skin and thus overcome the barrier function of the skin (35). So, we suspect that CPP$_{Tat}$ helped JDlys gain access to deeper tissue layers and prevent the skin damage caused by MRSA, although subcutaneous therapy is a complicated process involving integrated tissue consisting of numerous cell types besides keratinocytes. Fortunately, our study confirmed that treatment with CPP$_{Tat}$-JDlys could significantly reduce the number of MRSA bacteria in

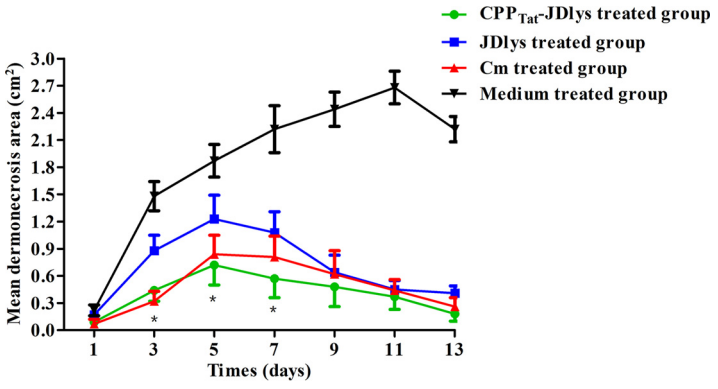

FIG 5 Progression of mean dermonecrotic area over 13 days in a mouse model of infection. The areas of the abscesses in each mouse flank were measured during the period of treatments. *, time points when the dermonecrotic areas treated with the medium buffer or JDlys were significantly greater ($P < 0.05$) than those treated with CPP$_{Tat}$-JDlys. The data shown are means ± SEMs from at least three independent experiments.

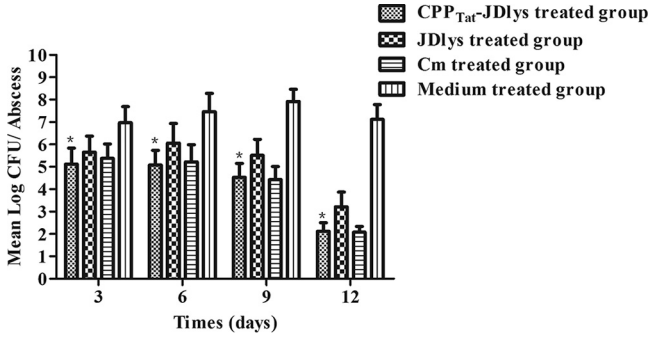

FIG 6 CPP-JDlys-mediated reduction in abscess burden, given as the number of CFU. Three mice were humanely sacrificed at preselected time points. Each lesion (two lesions per mouse) was aseptically excised and homogenized. *, time points when the burden (number of CFU) in lesions treated by CPP$_{Tat}$-JDlys was significantly lower ($P < 0.05$) than that in lesions treated with the medium buffer or JDlys. The data shown are means ± SEMs from at least three independent experiments.

cutaneous abscesses and shorten the course of wound healing compared with that required with JDlys treatment (Fig. 4 to 8). Furthermore, lysins as proteolytic enzymes, like other proteins introduced into mammalian organisms, are quickly cleared from the systemic circulation (36). So, continuous administration of CPP-JDlys (over a 3-day duration) was performed in order to maintain the enzymatic activity of the lysin, which then worked steadily in the cutaneous abscesses in the mice.

Meanwhile, the adverse effects of lysins *in vivo* have also been studied. Adverse effects are associated with bactericidal agents, including the release of large amounts of pathogen-associated molecular patterns that are recognized by Toll-like receptors and the induction of proinflammatory cytokines in mammals (37). However, our studies showed that no significant differences in the expression of proinflammatory cytokines were seen between uninfected mice treated with JDlys or CPP-JDlys and mice treated with PBS as a control over 12 days (Fig. 7). In addition, uninfected mice treated with either JDlys or CPP-JDlys did not show abscess formation (data not shown). Thus, it is suggested that there is no observable adverse effect of therapy with JDlys or CPP-JDlys. Moreover, it has been reported that lysin can stimulate the host to produce antibodies to influence its bactericidal activity *in vivo* (14). Unlike antibiotics or micromolecule antibacterial peptides, which are small and nonimmunogenic, lysins are peptides that stimulate the immune response, regardless of the way in which they are administered into the body, leading to the formation of antibodies that can reduce the activity of the lysin *in vivo* (14). However, Zhang et al. suggested that lysin antibodies do not affect the

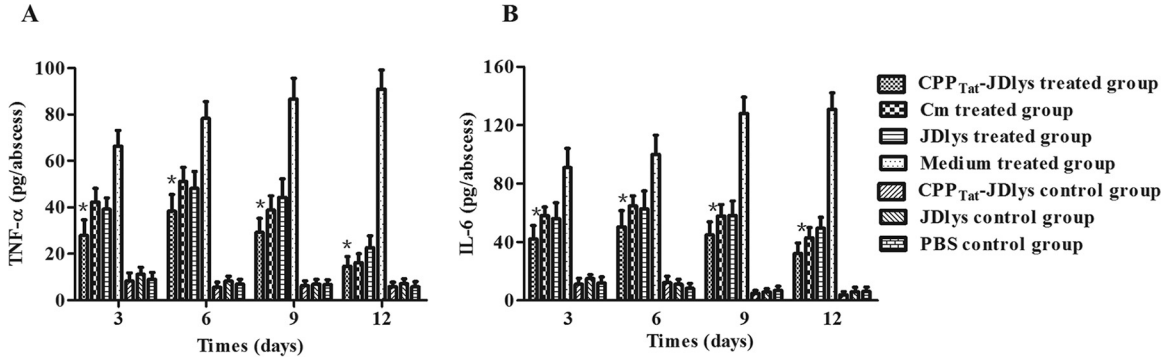

FIG 7 Systemic immune responses to CPP$_{Tat}$-JDlys in the mouse model. Supernatants from lesion homogenates were collected at different time points after treatment and assayed for TNF-α (A) and IL-6 (B) by ELISA. Three mice (two lesions per mouse) per group were sacrificed at each time point. Uninfected mice treated with JDlys, CPP$_{Tat}$-JDlys, and PBS were used to represent the CPP$_{Tat}$-JDlys, JDlys, and PBS control groups, respectively. Infected mice treated with PBS served as the medium-treated group. *, time points when the cytokine levels in lesions treated with CPP$_{Tat}$-JDlys were significantly lower ($P < 0.05$) than those in lesions treated with the medium buffer. The data shown are means ± SEMs from at least three independent experiments.

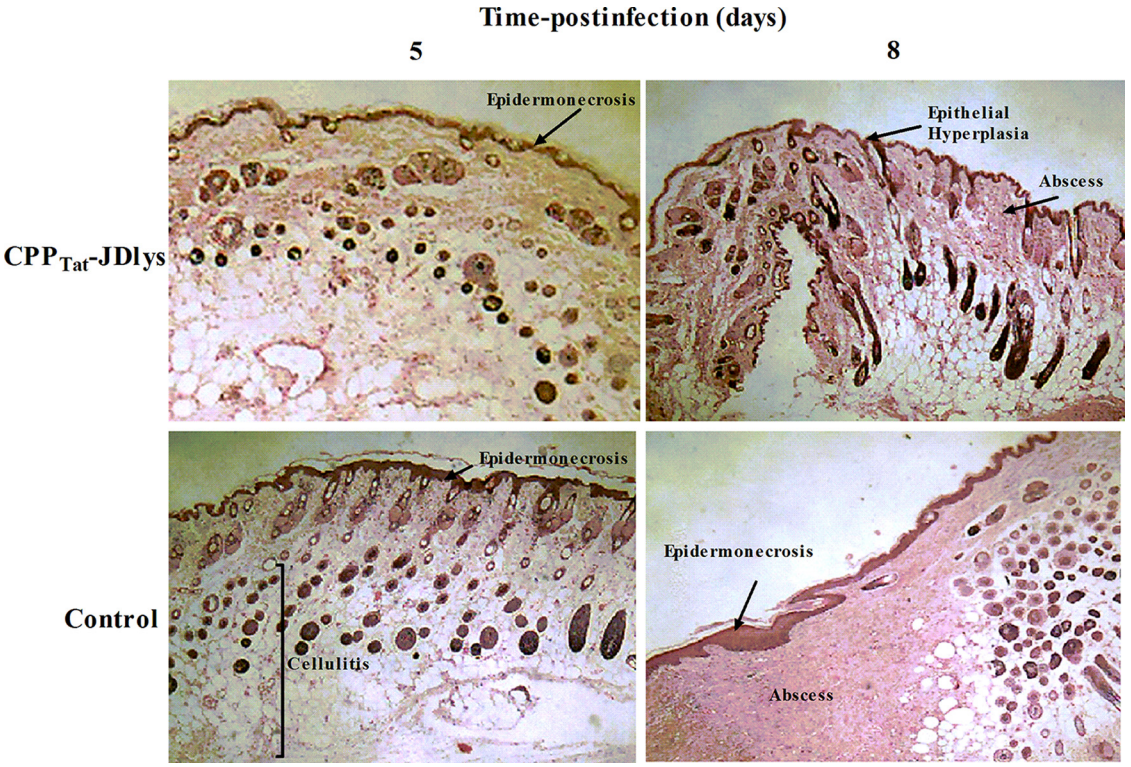

FIG 8 CPP$_{Tat}$-JDlys reduced MRSA-induced cutaneous abscesses and promoted the healing of skin lesions. BALB/c mice were infected with strain USA300 and treated with CPP$_{Tat}$-JDlys. Infected skin was collected from the animals at 5 and 8 days postinfection and processed for H&E staining and microscopic examination. Magnifications, ×10.

bactericidal efficacy of lysin *in vitro* or *in vivo* because the affinity of binding of the cell wall to lysin might be higher than the affinity of binding of antibodies to lysin (16). Our results also found that CPP-JDlys could maintain high levels of activity and continuously inhibit the survival of MRSA strains *in vivo*.

Collectively, our findings suggest that the fusion protein CPP-JDlys is a novel antimicrobial agent active against intracellular and skin infections caused by MRSA. So far, lysin still cannot replace antibiotics for clinical treatment (e.g., because of the narrow antibacterial spectrum [14]). However, the proper transformation of lysin could contribute to the better control of antibiotic-resistant bacteria as well as the development of a wider range of applications for antimicrobials.

MATERIALS AND METHODS

Ethics statement. The animal experiments were carried out according to animal welfare standards and approved by the Ethical Committee for Animal Experiments of Shanghai Jiao Tong University, Shanghai, China. All animal experiments complied with the guidelines of the Animal Welfare Council of China.

Bacterial strains, bacteriophage, and growth conditions. The bacteria used in this study are listed in Table 1. *Staphylococcus* strains were cultured aerobically in tryptic soy broth (TSB) or brain heart infusion (BHI) broth in a shaker (180 rpm) at 37°C. The bacterial burden, given as the number of CFU of *Staphylococcus*, was measured in BHI agar supplemented with 2% (vol/vol) fetal bovine serum (FBS; Gibco, Invitrogen Corp., Carlsbad, CA) under static conditions at 37°C. *Escherichia coli* strains, used for gene cloning and producing recombinant proteins, were cultured aerobically in Luria-Bertani (LB) broth with shaking (180 rpm) at 37°C. The JD007 phage was kindly provided by ZeLin Cui (Shanghai General Hospital, Shanghai, China) (25). Purification and genomic DNA extraction were performed as described previously (13).

Cloning, expression, and purification of JDlys and CPP-JDlys. The region encoding the lysin of phage JD007 (JDlys) was PCR amplified with primers 5′ BamHI_JDlys (CGCGGATCCATGGCTAAGACTCA AGCA, where the BamHI site is underlined) and 3′ XhoI_JDlys (CCGCTCGAGCTACTTGAATACTCCCCA, where the XhoI site is underlined), using the JD007 phage genome (GenBank accession number JX878671.1) as a template for JDlys. The PCR product was digested with BamHI/XhoI and cloned into the pET28a(+) vector. CPPs and linker sequences (Table 2) were identified by reverse translation into

nucleotide sequences (with an *E. coli* codon usage bias), followed by commercial synthesis (Sangon, Biotech Co., Ltd., Shanghai, China). The individual CPP sequences were inserted at the BamHI site (at the amino terminus of the JDlys sequence) or XhoI site (at the carboxy terminus of the JDlys sequence) of the pET28a(+) vector. Furthermore, green fluorescent protein (GFP; GenBank accession number LC336974.1) was synthesized (Sangon) and inserted at the BamHI site (at the amino terminus of the CPP_{Tat}-JDlys sequence) of the pET28a(+) vector. Constituted plasmids were expressed in *E. coli* BL21(DE3) grown to an optical density at 600 nm (OD_{600}) of 0.6 at 37°C, induced with 1 mM isopropyl-β-D-thiogalactoside (IPTG), and expressed for 12 h at 18°C. Cells were disrupted by sonication and purified by use of an Ni-Sepharose 6 Fast Flow resin gravity column (GE Healthcare BioSciences, Pittsburgh, PA, USA), as described previously (38). Moreover, for proteins used in cellular and murine experiments, endotoxins were removed by treatment with phosphate-buffered saline (PBS) containing a 0.1% Triton X-114 (Sigma-Aldrich, St. Louis, MO) elution of proteins on Ni-nitrilotriacetic acid columns (39).

Bactericidal activity of JDlys and CPP-JDlys. The MICs of JDlys or CPP-JDlys for multiple *Staphylococcus* strains were determined as described by Wiegand et al. with minor modifications (40). Briefly, *Staphylococcus* strains were freshly cultured to early exponential phase (OD_{600}, 0.2 to 0.4). The MIC was monitored by blending 100 μl of the bacterial suspension (diluted to 5×10^6 cells/ml) with 100 μl of the enzyme at different final concentrations (10, 20, 40, 80, 160, 320, and 640 μg/ml) in a 96-well microtiter plate. The plates were incubated for 20 h at 37°C and read with a 96-well plate reader (determination of the absorbance at 600 nm).

Determination of ability of bacteria to adhere to and invade HaCaT keratinocytes. HaCaT keratinocytes were grown in RPMI 1640 medium supplied with 10% FBS at 37°C in 5% CO_2. For the adhesion assay, keratinocytes were seeded into 12-well plates at a concentration of approximately 10^5 cells per well. On the next day, prepared bacterial strains were added to the keratinocytes at a multiplicity of infection (MOI) of 10. The plates were incubated for 60 min at 37°C in 5% CO_2. The keratinocytes were washed three times with PBS to remove nonadhered bacterial cells. After that, the keratinocytes were lysed with PBS containing 0.02% Triton X-100, and the adhered bacteria were quantified by serial dilution plating. The adhesion rate was calculated as follows: number of CFU of adhered bacteria/number of CFU of the initial number of bacteria.

For the invasion assay, keratinocytes were seeded into 12-well plates at a concentration of approximately 10^5 cells per well. On the next day, prepared bacterial strains were added to the keratinocytes at an MOI of 10. The plates were incubated for 60 min at 37°C in 5% CO_2. After that, the keratinocytes were washed three times with PBS, the medium was replaced with 1% FBS–RPMI 1640 medium containing 50 μg/ml of gentamicin to kill the extracellular *S. aureus* bacteria, and the keratinocytes were incubated for 60 min. After that, the keratinocytes were washed three times with PBS and then incubated for 15 min at 37°C in PBS with 0.02% Triton X-100 to lyse the keratinocytes and release the intracellular invading bacteria. The invasion rate was calculated as follows: number of CFU of invading bacteria/number of CFU of the initial number of bacteria.

CPP-JDlys-mediated intracellular *S. aureus* eradication assay. MRSA strain USA300 was cultured in BHI broth to exponential phase (about 1×10^9 CFU/ml) in a shaker at 37°C, harvested by centrifugation at 5,000 × *g* for 5 min, washed 3 times in PBS, and resuspended in fresh, serum-free RPMI 1640 medium without antibiotics. The keratinocyte monolayers were grown in 12-well tissue culture plates and infected with *S. aureus* cells (10^6 bacteria/well) at an MOI of 10 for 1 h at 37°C. Extracellular bacteria were removed by washing the keratinocytes 3 times with PBS, the medium was replaced with 1% FBS–RPMI 1640 medium containing 50 μg/ml of gentamicin to kill the extracellular *S. aureus* bacteria, and the keratinocytes were incubated for 1 h. Subsequently, the cells were washed 3 times with PBS to remove the gentamicin. This time point was defined as time zero. Equal volumes of purified JDlys (40 μg/ml [2× MIC]), CPP_{Tat}-JDlys (40, 80, 160, and 320 μg/ml [1×, 2×, 4×, and 8× MIC, respectively]), CPP_{Ant}-JDlys (320 μg/ml [2× MIC]), and CPP_{TP10}-JDlys (320 μg/ml [2× MIC]) proteins, commercial lysostaphin (40 μg/ml [2× MIC]; Sigma-Aldrich), vancomycin (5 μg/ml [2× MIC]; Sigma-Aldrich), chloramphenicol (Cm; 12.5, 25, 50, and 100 μg/ml [1×, 2×, 4×, and 8× MIC, respectively]), and PBS were added to cells that had been cleaned of gentamicin for 3 h. Cells were cultured throughout all experiments at 37°C in 5% CO_2. After that, infected cells were washed 3 times with PBS and then incubated for 15 min at 37°C with 0.02% Triton X-100 to lyse the keratinocytes and release the intracellular bacteria. Various dilutions of the lysates were plated on BHI agar plates and incubated overnight at 37°C. The colonies were counted to determine the number of intracellular bacteria. To analyze the number of surviving bacteria compared to the initial number of intracellular bacteria (time zero), the relative number of CFU (rCFU) was calculated as follows: number of CFU at 3 h/number of CFU at time zero (41).

Confocal microscopy of HaCaT keratinocytes. HaCaT keratinocytes were seeded onto uncoated 50-mm, glass-bottom dishes (MatTek Corporation, Ashland, MA) in RPMI 1640 medium supplemented with 5% (vol/vol) FBS at 37°C in 5% CO_2. After 12 h of culture, when the keratinocytes had about 90% coverage, the *S. aureus* USA300 cells were added and then incubated at 37°C for 1 h. After that, samples were washed 3 times with PBS, the medium was replaced with 1% FBS–RPMI 1640 medium containing 50 μg/ml of gentamicin to kill the extracellular *S. aureus* bacteria, and the keratinocytes were incubated for 1 h. Samples were then incubated with monoclonal mouse anti-*S. aureus* protein A (1:200; catalog number ab37644; Abcam, Cambridge, UK) for 30 min at 37°C. After that, samples were rinsed and incubated with goat anti-mouse IgG conjugated to tetramethyl rhodamine isocyanate (1:600; catalog number ab6786; Abcam) for 30 min at 37°C. After the washes, samples were exposed to 80 μg/ml of recombinant CPP-JDlys fused with GFP for 30 min. The keratinocytes were washed 3 times with PBS and then viewed using a confocal microscope (a Leica DM6000 CFS confocal fluorescence imaging micro-

TABLE 3 Primers used for qRT-PCR

Primer	Sequence (5′–3′)	Function
IL-6-F	AGCCTCAATGACGACCTA	A fragment for human IL-6 gene
IL-6-R	ATCTTTGTTGGAGGGTGA	
TNF-α-F	AGCCGCATCGCCGTCTCCTA	A fragment for human TNF-α gene
TNF-α-R	CAGCGCTGAGTCGGTCACCC	
β-actin-F	CCACGAAACTACCTTCAACTCC	A fragment for human β-actin gene
β-actin-R	GTGATCTCCTTCTGCATCCTGT	

scope on the Leica TCS-SP5 platform) at ×60 magnification. All fluorescence signals were collected on a photomultiplier after passage through appropriate filter sets.

LDH cytotoxicity assay. The cytotoxicity of the keratinocytes was detected by measuring the lactate dehydrogenase (LDH) activity present in the culture supernatant. A CytoTox 96 nonradioactive cytotoxicity assay (Promega, Madison, WI) was used according to the manufacturer's instructions. Briefly, keratinocytes were sampled at 3 h after treatment with JDlys, CPP-JDlys, and vancomycin as described above. Maximum release was achieved by lysing the monolayers with Triton X-100 at a final concentration of 1% (vol/vol). The activity of the enzymes was determined using a microplate reader (determination of the absorbance at 492 nm). The LDH released was designated that released spontaneously. Cytotoxicity was calculated as follows: percent cytotoxicity = (amount of LDH released in the test − amount released spontaneously)/(maximal amount released − amount released spontaneously).

Cytokine assays. To measure the cytokine levels of the infected keratinocytes, keratinocytes were sampled at 3 h after treatment with JDlys, CPP-JDlys, and vancomycin as described above. Total RNA was isolated from the supernatants of the keratinocytes using an AllPrep RNA microkit (Qiagen, West Sussex, UK). cDNA synthesis was performed using a PrimeScript RT reagent kit (TaKaRa, Dalian, China) according to the manufacturer's instructions. The mRNA levels were measured using a two-step relative quantitative reverse transcription-PCR (qRT-PCR). The β-actin housekeeping gene was amplified as an internal control. The sequences of the primers for tumor necrosis factor alpha (TNF-α), interleukin-6 (IL-6), and β-actin are listed in Table 3. Gene expression was normalized to the expression of the housekeeping gene β-actin. Real-time PCR was carried out using a SYBR Premix *Ex Taq* kit (TaKaRa) and a CFX Connect RT-PCR system (Bio-Rad, Hercules, CA, USA). The comparative cycle threshold ($2^{-\Delta\Delta CT}$) method was used to analyze the mRNA levels.

Murine model of cutaneous abscesses. BALB/c female mice aged 6 weeks were used for the subcutaneous abscess model as previously described by Ding et al. with minor modifications (42). In brief, mice were anesthetized, their flanks were shaved and sterilized, and the mice were randomized into appropriate study groups (20 mice in each group). Next, 50 μl of MRSA strain USA300 (5×10^7 CFU/flank) mixed with an equal volume of autoclaved Cytodex-1 beads (131 to 220 μm; Sigma-Aldrich) in PBS was injected subcutaneously. At 24 h postinfection, purified JDlys (50 μg/flank), CPP-JDlys (100 μg/flank), or chloramphenicol (100 μg/flank) was injected subcutaneously near the abscesses over the course of 3 days. CPP-JDlys alone (i.e., no bacteria) and medium (PBS buffer) were injected subcutaneously, and these mice served as control groups.

Abscess evaluation after therapy. (i) Abscess area. The areas of the abscesses in each mouse flank were measured during the period of treatment with JDlys, CPP-JDlys, Cm, and PBS buffer. To do so, the mice were anesthetized and the lesion site length and width were measured to quantify the abscess area (given in square centimeters).

(ii) Bacterial burden as number of CFU. The mice were humanely sacrificed at preselected time points after the treatments with JDlys, CPP-JDlys, Cm, and PBS buffer. Each flank was aseptically excised and homogenized. The suspension of abscesses was serially diluted in sterile PBS for quantitative culturing onto a BHI agar plate. All cultures were incubated (37°C) for 24 h, and the resulting colonies were enumerated as the number of CFU per abscess.

(iii) Cytokine quantification. Commercial enzyme-linked immunosorbent assay (ELISA) kits (Abcam) were used to examine the levels of the proinflammatory cytokines (i.e., TNF-α and IL-6) that were released from the abscess postinfection or after the treatments with CPP-JDlys, JDlys, Cm, and PBS buffer. The abscesses were excised, weighed, and homogenized as mentioned above. The cytokine levels were measured according to the manufacturer's instructions.

(iv) Histopathology analysis. The mice treated with CPP-JDlys or PBS were humanely sacrificed at 5 and 8 days postinfection. Abscess tissues were gently removed and immediately placed in 4% formalin. Formalin-fixed tissues were processed and stained with hematoxylin and eosin (H&E) and toluidine blue using a routine staining procedure and were subsequently analyzed using microscopy.

Statistical analyses. In all experiments, data points were plotted using GraphPad Prism (v.7.01) software (GraphPad Software, Inc., San Diego, CA). Data are presented as mean values ± standard errors of the means (SEMs). Related experiments were performed using the nonparametric Mann-Whitney U test. A P value of <0.05 was considered significant.

SUPPLEMENTAL MATERIAL

Supplemental material for this article may be found at https://doi.org/10.1128/AEM.00380-18.

SUPPLEMENTAL FILE 1, PDF file, 0.1 MB.

ACKNOWLEDGMENTS

This research was supported by the National Natural Science Foundation of China (grants 31672524, 31772744, and 31372500), the Key Project of Shanghai Municipal Agricultural Commission (grant 2016-6-2-1), the Agri-X Fund from Shanghai Jiao Tong University, the Science and Technology Commission of Shanghai Municipality (grants 16391903400 and 17391901400), and a grant from the Special Fund for Public Welfare Industry of the Chinese Ministry of Agriculture (201303041).

REFERENCES

1. Schittek B. 2011. The antimicrobial skin barrier in patients with atopic dermatitis. Curr Probl Dermatol 41:54–67. https://doi.org/10.1159/000323296.
2. Shahbazian JH, Hahn PD, Ludwig S, Ferguson J, Baron P, Christ A, Spicer K, Tolomeo P, Torrie AM, Bilker WB, Cluzet VC, Hu B, Julian K, Nachamkin I, Rankin SC, Morris DO, Lautenbach E, Davis MF. 22 September 2017. Multidrug and mupirocin resistance in environmental methicillin-resistant *Staphylococcus aureus* (MRSA) collected from the homes of people diagnosed with a community-onset (CO-) MRSA infection. Appl Environ Microbiol. https://doi.org/10.1128/AEM.01369-17.
3. Bitschar K, Wolz C, Krismer B, Peschel A, Schittek B. 2017. Keratinocytes as sensors and central players in the immune defense against *Staphylococcus aureus* in the skin. J Dermatol Sci 87:215–220. https://doi.org/10.1016/j.jdermsci.2017.06.003.
4. Kawasaki T, Kawai T. 2014. Toll-like receptor signaling pathways. Front Immunol 5:461. https://doi.org/10.3389/fimmu.2014.00461.
5. Skabytska Y, Kaesler S, Volz T, Biedermann T. 2016. The role of innate immune signaling in the pathogenesis of atopic dermatitis and consequences for treatments. Semin Immunopathol 38:29–43. https://doi.org/10.1007/s00281-015-0544-y.
6. Di Meglio P, Perera GK, Nestle FO. 2011. The multitasking organ: recent insights into skin immune function. Immunity 35:857–869. https://doi.org/10.1016/j.immuni.2011.12.003.
7. Soong G, Paulino F, Wachtel S, Parker D, Wickersham M, Zhang D, Brown A, Lauren C, Dowd M, West E, Horst B, Planet P, Prince A. 2015. Methicillin-resistant *Staphylococcus aureus* adaptation to human keratinocytes. mBio 6:e00289-15. https://doi.org/10.1128/mBio.00289-15.
8. Srisuwan S, Voravuthikunchai SP. 2017. Rhodomyrtus tomentosa leaf extract inhibits methicillin-resistant *Staphylococcus aureus* adhesion, invasion, and intracellular survival in human HaCaT keratinocytes. Microb Drug Resist 23:1002–1012. https://doi.org/10.1089/mdr.2016.0284.
9. Brinch KS, Sandberg A, Baudoux P, Van Bambeke F, Tulkens PM, Frimodt-Moller N, Hoiby N, Kristensen HH. 2009. Plectasin shows intracellular activity against *Staphylococcus aureus* in human THP-1 monocytes and in a mouse peritonitis model. Antimicrob Agents Chemother 53:4801–4808. https://doi.org/10.1128/AAC.00685-09.
10. Van Bambeke F, Carryn S, Seral C, Chanteux H, Tyteca D, Mingeot-Leclercq MP, Tulkens PM. 2004. Cellular pharmacokinetics and pharmacodynamics of the glycopeptide antibiotic oritavancin (LY333328) in a model of J774 mouse macrophages. Antimicrob Agents Chemother 48:2853–2860. https://doi.org/10.1128/AAC.48.8.2853-2860.2004.
11. Rivera AM, Boucher HW. 2011. Current concepts in antimicrobial therapy against select gram-positive organisms: methicillin-resistant *Staphylococcus aureus*, penicillin-resistant pneumococci, and vancomycin-resistant enterococci. Mayo Clin Proc 86:1230–1243. https://doi.org/10.4065/mcp.2011.0514.
12. Borysowski J, Lobocka M, Miedzybrodzki R, Weber-Dabrowska B, Gorski A. 2011. Potential of bacteriophages and their lysins in the treatment of MRSA: current status and future perspectives. BioDrugs 25:347–355. https://doi.org/10.2165/11595610-000000000-00000.
13. Wang Z, Zheng P, Ji W, Fu Q, Wang H, Yan Y, Sun J. 2016. SLPW: a virulent bacteriophage targeting methicillin-resistant *Staphylococcus aureus in vitro* and *in vivo*. Front Microbiol 7:934. https://doi.org/10.3389/fmicb.2016.00934.
14. Rios AC, Moutinho CG, Pinto FC, Del Fiol FS, Jozala A, Chaud MV, Vila MM, Teixeira JA, Balcao VM. 2016. Alternatives to overcoming bacterial resistances: state-of-the-art. Microbiol Res 191:51–80. https://doi.org/10.1016/j.micres.2016.04.008.
15. Yang H, Bi Y, Shang X, Wang M, Linden SB, Li Y, Li Y, Nelson DC, Wei H. 2016. Antibiofilm activities of a novel chimeolysin against *Streptococcus mutans* under physiological and cariogenic conditions. Antimicrob Agents Chemother 60:7436–7443. https://doi.org/10.1128/AAC.01872-16.
16. Zhang L, Li D, Li X, Hu L, Cheng M, Xia F, Gong P, Wang B, Ge J, Zhang H, Cai R, Wang Y, Sun C, Feng X, Lei L, Han W, Gu J. 2016. LysGH15 kills *Staphylococcus aureus* without being affected by the humoral immune response or inducing inflammation. Sci Rep 6:29344. https://doi.org/10.1038/srep29344.
17. Attai H, Rimbey J, Smith GP, Brown PJB. 2017. Expression of a peptidoglycan hydrolase from lytic bacteriophages Atu_ph02 and Atu_ph03 triggers lysis of *Agrobacterium tumefaciens*. Appl Environ Microbiol 83:e01498-17. https://doi.org/10.1128/AEM.01498-17.
18. Singh PK, Donovan DM, Kumar A. 2014. Intravitreal injection of the chimeric phage endolysin Ply187 protects mice from *Staphylococcus aureus* endophthalmitis. Antimicrob Agents Chemother 58:4621–4629. https://doi.org/10.1128/AAC.00126-14.
19. Fischetti VA. 2010. Bacteriophage endolysins: a novel anti-infective to control Gram-positive pathogens. Int J Med Microbiol 300:357–362. https://doi.org/10.1016/j.ijmm.2010.04.002.
20. Sulakvelidze A, Alavidze Z, Morris JG, Jr. 2001. Bacteriophage therapy. Antimicrob Agents Chemother 45:649–659. https://doi.org/10.1128/AAC.45.3.649-659.2001.
21. Johnson JL, Lowell BC, Ryabinina OP, Lloyd RS, McCullough AK. 2011. TAT-mediated delivery of a DNA repair enzyme to skin cells rapidly initiates repair of UV-induced DNA damage. J Investig Dermatol 131:753–761. https://doi.org/10.1038/jid.2010.300.
22. Liu C, Jiang K, Tai L, Liu Y, Wei G, Lu W, Pan W. 2016. Facile noninvasive retinal gene delivery enabled by penetratin. ACS Appl Mater Interfaces 8:19256–19267. https://doi.org/10.1021/acsami.6b04551.
23. Di Pisa M, Chassaing G, Swiecicki JM. 2015. Translocation mechanism(s) of cell-penetrating peptides: biophysical studies using artificial membrane bilayers. Biochemistry 54:194–207. https://doi.org/10.1021/bi501392n.
24. Copolovici DM, Langel K, Eriste E, Langel U. 2014. Cell-penetrating peptides: design, synthesis, and applications. ACS Nano 8:1972–1994. https://doi.org/10.1021/nn4057269.
25. Cui Z, Feng T, Gu F, Li Q, Dong K, Zhang Y, Zhu Y, Han L, Qin J, Guo X. 2017. Characterization and complete genome of the virulent Myoviridae phage JD007 active against a variety of Staphylococcus aureus isolates from different hospitals in Shanghai, China. Virol J 14:26. https://doi.org/10.1186/s12985-017-0701-0.
26. Sinha B, Herrmann M. 2005. Mechanism and consequences of invasion of endothelial cells by *Staphylococcus aureus*. Thromb Haemost 94:266–277.
27. Hsu CY, Yang SC, Sung CT, Weng YH, Fang JY. 2017. Anti-MRSA malleable liposomes carrying chloramphenicol for ameliorating hair follicle targeting. Int J Nanomedicine (Lond) 12:8227–8238. https://doi.org/10.2147/IJN.S147226.

28. Miller LS, Cho JS. 2011. Immunity against *Staphylococcus aureus* cutaneous infections. Nat Rev Immunol 11:505–518. https://doi.org/10.1038/nri3010.
29. Mohamed MF, Abdelkhalek A, Seleem MN. 2016. Evaluation of short synthetic antimicrobial peptides for treatment of drug-resistant and intracellular *Staphylococcus aureus*. Sci Rep 6:29707. https://doi.org/10.1038/srep29707.
30. Poovelikunnel T, Gethin G, Humphreys H. 2015. Mupirocin resistance: clinical implications and potential alternatives for the eradication of MRSA. J Antimicrob Chemother 70:2681–2692. https://doi.org/10.1093/jac/dkv169.
31. Carryn S, Chanteux H, Seral C, Mingeot-Leclercq MP, Van Bambeke F, Tulkens PM. 2003. Intracellular pharmacodynamics of antibiotics. Infect Dis Clin North Am 17:615–634. https://doi.org/10.1016/S0891-5520(03)00066-7.
32. Gu J, Feng Y, Feng X, Sun C, Lei L, Ding W, Niu F, Jiao L, Yang M, Li Y, Liu X, Song J, Cui Z, Han D, Du C, Yang Y, Ouyang S, Liu ZJ, Han W. 2014. Structural and biochemical characterization reveals LysGH15 as an unprecedented "EF-hand-like" calcium-binding phage lysin. PLoS Pathog 10:e1004109. https://doi.org/10.1371/journal.ppat.1004109.
33. Hermoso JA, Garcia JL, Garcia P. 2007. Taking aim on bacterial pathogens: from phage therapy to enzybiotics. Curr Opin Microbiol 10:461–472. https://doi.org/10.1016/j.mib.2007.08.002.
34. Edwards AM, Potter U, Meenan NA, Potts JR, Massey RC. 2011. *Staphylococcus aureus* keratinocyte invasion is dependent upon multiple high-affinity fibronectin-binding repeats within FnBPA. PLoS One 6:e18899. https://doi.org/10.1371/journal.pone.0018899.
35. Wang Y, Wang S, Shi P. 2016. Transcriptional transactivator peptide modified lidocaine-loaded nanoparticulate drug delivery system for topical anesthetic therapy. Drug Deliv 23:3193–3199. https://doi.org/10.3109/10717544.2016.1160459.
36. Loeffler JM, Djurkovic S, Fischetti VA. 2003. Phage lytic enzyme Cpl-1 as a novel antimicrobial for pneumococcal bacteremia. Infect Immun 71:6199–6204. https://doi.org/10.1128/IAI.71.11.6199-6204.2003.
37. Kelesidis T. 2014. The interplay between daptomycin and the immune system. Front Immunol 5:52. https://doi.org/10.3389/fimmu.2014.00052.
38. Zhang H, Zhang C, Wang H, Yan YX, Sun J. 2016. A novel prophage lysin Ply5218 with extended lytic activity and stability against *Streptococcus suis* infection. FEMS Microbiol Lett 363:fnw186. https://doi.org/10.1093/femsle/fnw186.
39. Reichelt P, Schwarz C, Donzeau M. 2006. Single step protocol to purify recombinant proteins with low endotoxin contents. Protein Expr Purif 46:483–488. https://doi.org/10.1016/j.pep.2005.09.027.
40. Wiegand I, Hilpert K, Hancock RE. 2008. Agar and broth dilution methods to determine the minimal inhibitory concentration (MIC) of antimicrobial substances. Nat Protoc 3:163–175. https://doi.org/10.1038/nprot.2007.521.
41. Wang Z, Guo C, Xu Y, Liu G, Lu C, Liu Y. 2014. Two novel functions of hyaluronidase from *Streptococcus agalactiae* are enhanced intracellular survival and inhibition of proinflammatory cytokine expression. Infect Immun 82:2615–2625. https://doi.org/10.1128/IAI.00022-14.
42. Ding Y, Fu Y, Lee JC, Hooper DC. 2012. *Staphylococcus aureus* NorD, a putative efflux pump coregulated with the Opp1 oligopeptide permease, contributes selectively to fitness *in vivo*. J Bacteriol 194:6586–6593. https://doi.org/10.1128/JB.01414-12.